ACS Combinatorial Science

LETTER

pubs.acs.org/acscombsci

Genetic Algorithm-Assisted Optimization of Nanoporous TiO_2 for Low-Temperature Processable Photoanodes of Dye-Sensitized Solar Cells

Soyoung Kim, Kee-Sun Sohn,* and Myoungho Pyo*

Department of Printed Electronics and Engineering in World Class University (WCU) Program, Sunchon National University, Sunchon, Chonnam 540-742, Republic of Korea

Supporting Information

ABSTRACT: Genetic algorithm (GA), a promising optimization process in Heuristics, has proven to be a powerful tool in controlling the nanostructure of low-temperature processable photoanodes in dye-sensitized solar cells (DSSC). For photoanodes that are composed of various sizes of TiO_2 nanoparticles and multiwalled carbon nanotubes in a double-layer configuration, the best composition was determined based on the objective functions of cell efficiency (η) and its variance. The latter function was chosen since TiO_2 dispersions with no organic binders often aggravated the efficiency of reproducibility. From a total of 64,536 cases, 24 different cases (6 samples prepared for each composition) per generation were selected, and their objective functions were compared. GA was effective in the optimization of photoanodes, and resulted in a cell efficiency of 7.3 ± 0.2% with a short circuit current of 13.8 ± 0.4 mA cm^{-2}, an open circuit voltage of 0.737 ± 0.006 V, and a fill factor of 71.8 ± 0.6% after 3 generations. The η of 7.3 ± 0.2% is the highest value for low-temperature processable dye-sensitized solar cells prepared without further treatment of TiO_2 films to enhance interparticle connections.

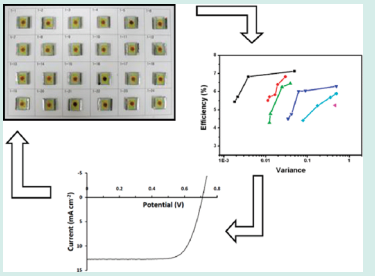

KEYWORDS: genetic algorithm, dye-sensitized solar cell, photoanode

Beginning with the pioneering work by Grätzel and O'Regan in 1991,[1] dye-sensitized solar cells (DSSCs) have been under extensive research and development.[2] As a result, single cells showing about 10% power conversion efficiency (η) can be routinely prepared under ambient conditions. To successfully market DSSCs by replacing the current solar energy devices or electric power sources, however, other aspects other than a high η must be taken into account. The development of a low-temperature process for TiO_2 films is one of the important aspects since it enables the fabrication of flexible DSSCs on a plastic substrate via printing, which opens up new applications for DSSCs.[3]

The exclusion of a high-temperature sintering procedure for TiO_2 films does not allow for the usage of polymeric binders. This inevitably leads to difficulties in the formation of interparticle connections in TiO_2 as well as for the control of pore sizes, which results in slow electron transport through TiO_2 films and/or inconsistent I_3^- diffusion through an electrolyte medium. To circumvent this barrier, various strategies such as the incorporation of TiO_2 nanotubes,[4] the mechanical compression of TiO_2 films,[5] and the electrophoretic deposition of TiO_2[6] have been reported via a low-temperature process. Arakawa et al. dealt with the η of 7.6% by pressurizing TiO_2 films,[5a] but the typical performances of low-temperature DSSCs with no post-treatment of TiO_2 films are still far lower than those of conventional high-temperature DSSCs.[7] The incorporation of multiwalled carbon nanotubes (MWNT) into TiO_2 also has been investigated, and it has revealed that the η of low-temperature DSSCs can be increased up to 5.02% at 0.1 wt % MWNT loading.[8] However, the involvement of the aforementioned additional treatments would countermand the merit of a low-temperature process in terms of cost savings. In this regard, the aim here was to develop a DSSC with an η that is greater than those reported thus far by excluding all additional processes with the exception of optimizing TiO_2 composition.

Despite the importance of a low-temperature process for TiO_2 nanostructures, no previous work has comprehensively investigated the effect of TiO_2 composition on the performance of low-temperature DSSCs. This may be because it has generally been assumed that the optimal TiO_2 composition accomplished through a high-temperature process was also valid for low-temperature DSSCs. That is not the case, however, since TiO_2 produced under low-temperature possesses loosely interconnected TiO_2 particles, which leads to inferior electron transport properties. Therefore, the optimization of nanostructures for a low-temperature TiO_2 may be of more importance than it is for a high-temperature TiO_2. The high-temperature TiO_2 nanostructure that has been extensively investigated by many research groups for the past several decades is already considered to be optimized.[9] However, the development of low-temperature TiO_2 nanostructures is in the early stages and has received less attention, with the exception of the incorporation of one-dimensional

Received: September 14, 2010
Revised: December 13, 2010
Published: January 05, 2011

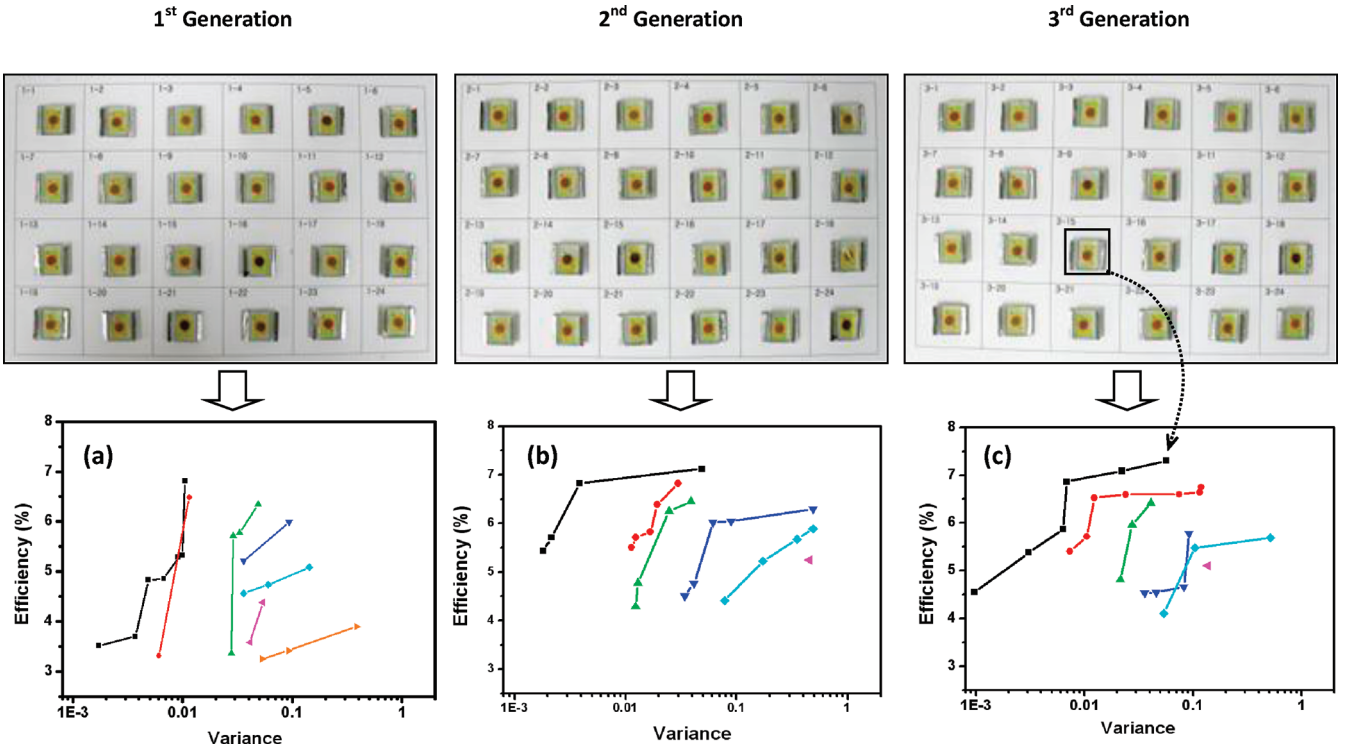

Figure 1. Pareto frontiers obtained for each generation by plotting η versus variance graphs and photographs of (a) 1st, (b) 2nd, and (c) 3rd generation. Each Pareto frontier is shown in a unique color, e.g., 1st and 2nd Pareto frontiers are shown in black and red, respectively, and data points are also shown to illustrate niche sharing.

nanostructures.[4,8] Accordingly, it would take a long time to optimize a low-temperature TiO_2 nanostructure if the procedure for a high-temperature TiO_2 nanostructure were used.

Rather than optimize low-temperature TiO_2 by standard trial-and-error methods, we adopted genetic algorithm and pseudo high-throughput processes to make it possible to optimize a low-temperature TiO_2 nanostructure in a relatively short time frame. Genetic algorithm (GA) is one of the most efficient stochastic optimization strategies employed to solve multidimensional problems,[10] and has been previously used to develop new materials and catalysts.[11] For instance, we have identified luminescent multicompositional inorganic compounds using a GA-assisted combinatorial materials search (GACMS).[11e,11f] For the optimization of low-temperature TiO_2 nanostructures we designed a processing parameter space consisting of 65,536 discrete combinatorial sets. The processing parameters were the size and composition of TiO_2 nanoparticles, the fraction of MWNT, and the volume of solvent in a bilayer structure (for details, see the Experimental Procedures section and the Supporting Information). Because it is not possible to track all the 65,536 possible combinations, the use of GA was necessary to optimize processing conditions and reach a maximum η.

Error-free experimental processes are also very important in GACMS because evaluation of an unknown objective function is performed only by actual experimentation, such as synthesis, and by subsequent characterization or measurement. Experimental evaluation of an unknown objective function (η in this case) always gives rise to experimental error or inconsistency. Thus, it is reasonable to regard the variance of measured objective function values as a function of the decision parameters (processing parameters in this case). In the present study, therefore, the variance was considered to be an unknown objective function that should be minimized during the GACMS process. A new strategy was required to handle two different objective functions simultaneously, the materials property of concern (η in this case) and its variance. Non-dominated sorting genetic algorithm (NSGA)[12] enabled determination of this issue in a systematic way. In this regard, we used an NSGA-assisted combinatorial materials search (NSGACMS) to simultaneously minimize variance and to maximize η and thereby to get a set of optimized nanostructures for TiO_2 at low temperature. The NSGA process involving both the material properties and the experimental inconsistency (variance in this case) was described in greater detail in our previous report.[11e,11f]

The randomly chosen 24 compositions for the first generation were iteratively processed 6 times. The η values of 6 duplicate films for each composition were measured, and the average and the variance of the η's were processed for the 4 highest samples out of the 6. This was done because we occasionally (at most 2 out of 6 duplicates) observed very low efficiency values, which were below half of the average of the others. We assumed that this sort of failure was mostly due to experimental error. Therefore, we uniformly skipped 2 samples from every case for the sake of systematic comparisons, hoping to eliminate the vast majority of the erroneous measurements. The observed variance was then assumed to originate mostly from intrinsic inconsistencies, defined as an error that could be neither easily identified nor controlled.[11e,11f]

An important issue for NSGA is Pareto optimality,[12a] which determines the relative dominance of the η and the variance. The goal of multiobjective optimization is to find a set of non-dominated solutions (ideally with a good spread) by use of

dx.doi.org/10.1021/co1000025 |ACS Comb. Sci. 2011, 13, 101–106

GA. For this purpose, Srinivas and Deb[12a] proposed NSGA, which is based on several layers of classification for the individuals. The main purpose of NSGA is to obtain the first Pareto frontier that is located in a more promising area and more widely and evenly spread. In this respect, it is clear that our NSGA succeeded, as described below. NSGA does not involve the pursuit of a weighted sum of two objective functions; rather, its purpose is the simultaneous optimization of two objective functions to find a group of solutions (the first Pareto) in a wide range.

Prior to the selection process, the population was ranked based on dominance (using Pareto sorting or ranking); all nondominated individuals were classified into one category with a dummy fitness value. Pareto sorting designates the iterative elimination of the Pareto frontier from the total population until nothing remains. Through this process, NSGA yielded the second and third generations, and the Pareto-sorted results are shown in Figures 1 (b) and (c), respectively. It should be noted that we had a quite high η even in the randomly chosen first generation, which amounted to 6.8%. This indicated that a stochastic process compensated for the limitations of any knowledge-based trial errors. Starting with such an unexpectedly high value, the η evolved further as it progressed to later generations. After 3 generations, DSSCs showing an η of 7.3 $\pm$ 0.2% with a variance of 0.06 were constructed (sample 3−15), implying that our NSGACMS process worked properly. The overall variance range that we experienced in the entire NSGACMS process was acceptable.

For samples 3−15, the short circuit current (J_{sc}), the open circuit voltage (V_{oc}), and the fill factor (ff) were 13.8 $\pm$ 0.4 mA cm^{-2}, 0.737 $\pm$ 0.006 V, and 71.8 $\pm$ 0.6%, respectively. The η value of 7.3 $\pm$ 0.2% is the highest value to be reported for low-temperature processable photoanodes prepared with no further treatment of TiO_2 to enhance interparticle connections (e.g., pressurization[5] or UV/ozone treatment[13]). The bottom layers for samples 3−15 were composed of 0.85 g of 21 nm TiO_2, 0.15 g of 140 nm TiO_2, and 0.1 mg MWNT and the top layers were composed only of 1.0 g of 21 nm TiO_2. The change of objective functions with each generation are described in Supporting Information.

The J-V curves for the DSSCs with the highest η at each generation are presented in Figure 2. The curves were taken from the samples possessing the second highest η among the 6 duplicates, which was close to the average values for cell parameters. Both J_{sc} and V_{oc} were improved with each iterative generation, J_{sc} going from 12.7 to 14.2 mA cm^{-2} and V_{oc} was increased from 0.71 to 0.74 V. On the other hand, ff slightly decreased from 76.5 to 71.1%, resulting in an increase of η from 6.91 to 7.45%.

Figure 3 shows the FESEM sectional image of the photoanode prepared from 0.85 g 21 nm of TiO_2, 0.15 g of 140 nm TiO_2, and 0.1 mg of MWNT dispersed in 8.0 mL of ethanol for the bottom and 1.0 g of 21 nm TiO_2 in 20 mL of ethanol for the top (sample 3−15). The bottom and top layers were about 9.2 and 3.1 μm thick, respectively. In all generations, the thicknesses ranged from 3 to 10 μm for the bottom and 3.0−3.5 μm for the top, depending on the TiO_2 compositions and the volume of ethanol. Figure 3 also shows that 140 nm of TiO_2 and MWNT were well dispersed in the bottom layer. Note that MWNT exists as a single strand with no formation of bundles. The magnified view in Figure 3c indicates the presence of a single nanotube, the diameter of which was similar to that of MWNT (25 nm).

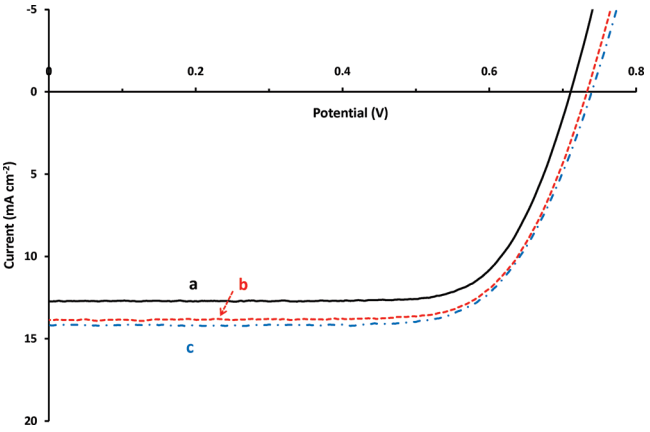

Figure 2. J-V curves for the composition of the highest η at (a) 1st, (b) 2nd, and (c) 3rd generation. η(%), J_{sc} (mA cm^{-2}), V_{oc} (V), and ff (%) were 6.91, 12.7, 0.71, and 76.5 and 7.34, 13.9, 0.73, 72.3 for (b), and 73.7 $\pm$ 0.9 for (a) and 7.45, 14.2, 0.74, and 71.1 for (c).

Figure 3 suggests that a homogeneous TiO_2 dispersion was maintained within the time duration of TiO_2 film preparation, which is a critical factor for the reproducible production of TiO_2 film.

The inclusion of a MWNT of 0.01 wt %, relative to the total mass of TiO_2 (1.0 g) in samples 3−15, was not surprising. It is generally accepted that a well-dispersed MWNT at an appropriate concentration improves electron transport.[14] The reported values for the low-temperature DSSCs ranged within a few hundredths wt %.[8] This was also the case in our double-layer configuration as the electrochemical impedance spectroscopic results show in Figure 4. It is well-known that the middle semicircle is related to the back electron transfer for the TiO_2/dye/electrolyte interface and for electron transport resistance through TiO_2.[15] Although the latter can be ignored at V_{oc} in conventional DSSCs, the lack of sufficient interconnection for low-temperature TiO_2 makes it significant.[16] Figure 4 is consistent with this situation, showing that the dc resistance of middle semicircles was reduced from 23 Ω to 15 Ω for DSSCs prepared (a) with and (b) without MWNT.

Unexpectedly, while the bottom layer of sample 3−15 contained 15 wt % 140 nm TiO_2, the top layer consisted of 21 nm TiO_2 only. This stands in contrast to the usual incorporation of large-particle TiO_2 into a top layer for light scattering during high-temperature synthesis.[17] The reason for this temperature-dependent difference between TiO_2 particle sizes is not clear at this point, but it appears to imply that the dominant factor determining η in low-temperature TiO_2 is electron transport. Note that the photoanode of samples 1−21 (the highest η in first generation) also did not contain large TiO_2 particles in the top layer. We are currently investigating the reasons for this difference in greater detail.

In summary, we applied NSGA for the first time in the optimization of photoanode compositions in a low-temperature process. The results showed that NSGA worked successfully for the simultaneous optimization of η and its variance. After 3 generations, the best cell revealed an η of 7.3 $\pm$ 0.2%, which is the highest ever reported with no post-treatment of TiO_2 films. The optimal composition of MWNT in the bottom layer and the optimal thickness of the TiO_2 film (bottom and top) were similar to that found in high-temperature processing, but the content of 140 nm TiO_2 was quite different from conventional expectations.

dx.doi.org/10.1021/co1000025 |ACS Comb. Sci. 2011, 13, 101–106

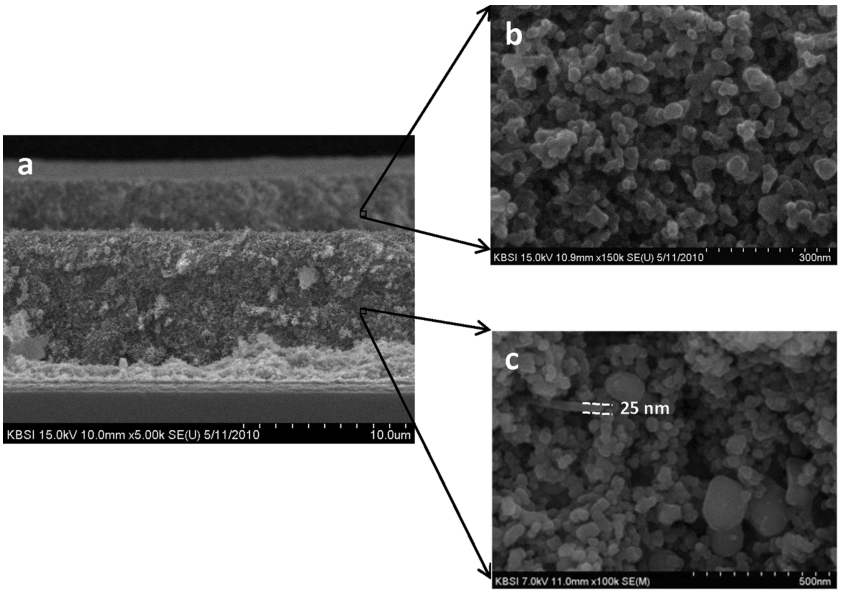

Figure 3. FESEM images for a section of sample 3−15. The layer thickness of the bottom and the top are about 9.2 and 3.1 μm, respectively.

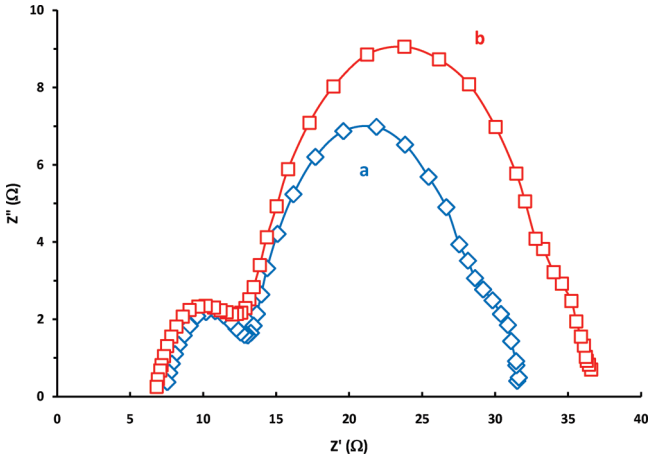

Figure 4. Electrochemical impedance spectra of DSSCs composed of photoanodes of (a) sample 3−15 and (b) MWNT-removed sample 3−15 in the bottom layer.

The best composition was obtained with a bottom layer containing 0.01 wt % MWNT and 15 wt % 140 nm TiO_2 and with a top layer of only 21 nm TiO_2.

EXPERIMENTAL PROCEDURES

A predetermined amount of 21 nm (Degussa), 140 nm (Aldrich), and 210 nm (Cosmo Chem., Korea) of TiO_2 were dispersed in ethanol and mixed with 1.0 mL of ethanol containing COOH-functionalized MWNT (Nanostructured & Amorphous Materials Inc., 10−20 nm outer diameter, 10−30 μm length, and 1.9−2.1% functionalization). The average particle size of TiO_2 was determined using Scherrer's equation from X-ray diffraction. Titanium(IV) isopropoxide (Aldrich, TTIP) of 0.08 mol was added to a TiO_2/MWNT mixture in ethanol, containing 1.00 g of TiO_2. The film thickness was controlled by using ethanol to change the solid content of dispersions. A double layer configuration was produced using the doctor blade method. Immediately after tip sonication of the mixture for 10 min, the bottom layer was first coated on a cleaned FTO, which was followed by a top layer coating on the completely dried TiO_2 bottom layer.

The TiO_2 compositions of bottom layers were varied ranging from 0.7 g ∼ 1.0 g for 21 nm and 0.0 g ∼ 0.3 g for both 140 and 210 nm particles for a total of 1.0 g. TiO_2 mixtures were added to different volumes of ethanol (6 mL ∼ 20 mL). TTIP of 0.290 mL and MWNT of various amounts were added into TiO_2-dispersed ethanol. The greatest content of MWNT was limited to 2 mg. The total number of cases for the bottom layer was 512 (2^8). The TiO_2 compositions for top layers were also varied in a wider range. The contents of 3 kinds of TiO_2 were all allowed to change from 0.0 g ∼ 1.0 g, maintaining a total TiO_2 of 1.0 g. The procedure for the bottom layer was repeated with a constant volume of ethanol (20.0 mL). The detailed decision parameters presented in Supporting Information indicate a total number of cases of 65,536 (2^8 and 2^7 for the bottom and the top, respectively). This means that, without the aid of a statistical tool, a total number of samples of more than a few hundred thousand should be prepared to determine the optimal composition since multiple cells for each composition are required to establish consistency.

The counter electrode was prepared by applying 2 drops of 5 mM H_2PtCl_6 on FTO and by sintering at 400 °C for 15 min. The Pt counter and TiO_2 electrodes were assembled face-to-face, using hot melting foil (Solaronix SX1170−60) sandwiched between two electrodes. The space between the electrodes was filled with an electrolyte solution through two holes. The two holes were then completely sealed using Surlyn film and cover glass. The electrolyte solution contained 0.2 M lithium iodide, 0.05 M iodine, 0.5 M *t*-butylpyridine, and 0.7 M 1,2-dimethyl-3-propylimidazolium iodide in acetonitrile. The mask of a hole that was slightly larger (0.283 cm^2) than the active area of N3/TiO_2 (0.196 cm^2) was affixed to the photoanode side.

The J-V characteristics of DSSCs were measured under simulated AM 1.5 solar illumination with 100 mW cm^{-2} (300 W Xenon lamp, Oriel Instruments). Electrochemical impedance spectroscopy (EIS) of DSSCs was carried out using a potentiostat/galvanostat (PARSTAT 2273). The EIS spectra were recorded

over a frequency range of 100 kHz to 0.1 Hz. An AC amplitude of ±10 mV was applied using open-circuit voltage under irradiation. Film thickness was measured using a FESEM (Hitachi S4800) and a profilometer (Tencor Alpha-step 500).

■ ASSOCIATED CONTENT

Supporting Information. The processing parameter design and the list of detailed processing parameters, and objective functions (η and variance) for each generation. This material is available free of charge via the Internet at http://pubs.acs.org.

■ AUTHOR INFORMATION

Corresponding Author

*Phone: (61) 750-3557. Fax: (61) 750-5260. E-mail: kssohn@sunchon.ac.kr (K.-S.S.), mho@sunchon.ac.kr (M.P.).

Author Contributions

M.P. and K.-S.S. designed the experiments. S.K. and M.P. performed the experiments. K.-S.S. coded computational programs and performed the computations. K.-S.S. and M.P. co-wrote the manuscript and the Supporting Information.

Funding Sources

This research was supported by the WCU (World Class University) program at Sunchon National University.

■ REFERENCES

(1) B. O'Regan, B.; Grätzel, M. A Low-cost, High-efficiency Solar Cell Based on Dye-sensitized Colloidal TiO_2 Films. *Nature* **1991,** *353,* 737–740.

(2) (a) Saji, V. S.; Zong, K.; Pyo, M. J. NIR-absorbing Poly(thieno-[3,4-*b*]thiophene-2-carboxylic acid) as a Polymer Dye for Dye-sensitized Solar Cells. *Photochem. Photobiol. A: Chem.* **2010,** *212,* 81–87. (b) Wang, J.; Lin, Z. Dye-sensitized TiO_2 Nanotube Solar Cells with Markedly Enhanced Performance via Rational Surface Engineering. *Chem. Mater.* **2010,** *22,* 579–584. (c) Grätzel, M. Photoelectrochemical Cells. *Nature* **2001,** *414,* 338–344.

(3) Hsu, C.-P.; Lee, K.-M.; Huang, J. T.-W.; Lin, C.-Y.; Lee, C.-H.; Wang, L.-P.; Tsai, S.-Y.; Ho, K.-C. EIS Analysis on Low Temperature Fabrication of TiO_2 Porous Films for Dye-sensitized Solar Cells. *Elctrochim. Acta* **2008,** *53,* 7514–7522.

(4) Xiao, Y.; Wu, J.; Yue, G.; Xie, G.; Lin, J.; Huang, M. The Preparation of Titania Nanotubes and Its Application in Flexible Dye-sensitized Solar Cells. *Electrochim. Acta* **2010,** *55,* 4573–4578.

(5) (a) Yamaguchi, T.; Tobe, N.; Matsumoto, D.; Nagai, T.; Arakawa, H. Highly Efficient Plastic-Substrate Dye-sensitized Solar Cells with Validated Conversion Efficiency of 7.6%. *Sol. Energy Mater. Sol. Cells* **2010,** *94,* 812–816. (b) Yamaguchi, T.; Tobe, N.; Matsumoto, D.; Arakawa, H. Highly Efficient Plastic Substrate Dye-sensitized Solar Cells Using a Compression Method for Preparation of TiO_2 Photoelectrodes. *Chem. Commun.* **2007,** 4767–4769.

(6) Miyasaka, T.; Kijitori, Y. Low-Temperature Fabrication of Dye-sensitized Plastic Electrodes by Electrophoretic Preparation of Mesoporous TiO_2 Layers. *J. Electrochem. Soc.* **2004,** *151,* A1767–A1773.

(7) Agrios, A. G.; Hagfeldt, A. Low-temperature TiO_2 Films for Dye-sensitized Solar Cells: Factors Affecting Energy Conversion Efficiency. *J. Phys. Chem. C* **2008,** *112,* 10021–10026.

(8) Lee, K.-M.; Hu, C.-W.; Chen, H.-W.; Ho, K.-C. Incorporating Carbon Nanotube in a Low-Temperature Fabrication Process for Dye-sensitized TiO_2 Solar Cells. *Sol. Energy Mater. Sol. Cells* **2008,** *92,* 1628–1633.

(9) (a) Kim, Y. J.; Lee, M. H.; Kim, H. J.; Lim, G.; Choi, Y. S.; Park, N.-G.; Kim, K.; Lee, W. I. Formation of Highly Efficient Dye-Sensitized Solar Cells by Hierarchical Pore Generation with Nanoporous TiO_2 Spheres. *Adv. Mater.* **2009,** *21,* 3668–3673. (b) Lee, K.-M.; Suryanarayanan, V.; Ho, K.-C. Influences of Different TiO_2 Morphologies and Solvents on the Photovoltaic Performance of Dye-sensitized Solar Cells. *J. Power Sources* **2009,** *188,* 635–641. (c) Wang, Z.-S.; Kawauchi, H.; Kashima, T.; Arakawa, H. Significant Influence of TiO_2 Photoelectrode Morphology on the Energy Conversion Eefficiency of N719 Dye-sensitized Solar Cell. *Coord. Chem. Rev.* **2004,** *248,* 1381–1389.

(10) (a) Holland, J. H. *Adaption in Natural and Artificial System*; University of Michigan Press: Ann Arbor, MI, 1975. (b) Goldberg, D. E. *Genetic Algorithm in Search, Optimization, and Machine Learning*; Addison-Wesley: Reading, MA, 1989. (c) Forrest, S. Genetic Algorithms: Principles of Adaptation Applied to Computation. *Science* **1993,** *261,* 872–878.

(11) (a) Rodemerck, U.; Baerns, M.; Holena, M.; Wolf, D. Application of a Genetic Algorithm and a Neural Network for the Discovery and Optimization of New Solid Catalytic Materials. *Appl. Surf. Sci.* **2004,** *223,* 168–174. (b) Pereira, S. R. M.; Clerc, F.; Farrusseng, D.; Vander waal, J. C.; Mashmeyer, T. Effect of the Genetic Algorithm Parameters on the Optimisation of Heterogeneous Catalysts. *QSAR Comb. Sci.* **2005,** *24,* 45–57. (c) Serra, J. M.; Corma, A.; Valero, S.; Argente, E.; Botti, V. Soft Computing Techniques Applied to Combinatorial Catalysis: A New Approach for the Discovery and Optimization of Catalytic Materials. *QSAR Comb. Sci.* **2007,** *26,* 11–26. (d) Bulut, M.; Gevers, L. E. M.; Paul, J. S.; Vankelecom, I. F. J.; Jacobs, P. A. Directed Development of High-Performance Membranes via High-Throughput and Combinatorial Strategies. *J. Comb. Chem.* **2006,** *8,* 168–173. (e) Sharma, A. K.; Kulshreshtha, C.; Sohn, K.; Sohn, K. -S. Systematic Control of Experimental Inconsistency in Combinatorial Materials Science. *J. Comb. Chem.* **2009,** *11,* 131–137. (f) Sharma, A. K.; Kulshreshtha, C.; Sohn, K. -S. Discovery of New Green Phosphors and Minimization of Experimental Inconsistency Using a Multi-Objective Genetic Algorithm-Assisted Combinatorial Method. *Adv. Funct. Mater.* **2009,** *19,* 1705–1712.

(12) (a) Srinivas, N.; Deb, K. Multiobjective Optimization Using Nondominated Sorting in Genetic Algorithms. *Intl. J. EVol. Comput.* **1994,** *2,* 221–248. (b) Deb, K.; Goldberg, D. E. An Investigation of Niche and Species Formation in Genetic Function Optimization In *Proceedings of the Third International Conference on Genetic Algorithms*; Schaffer, J. D., Ed.; Morgan Kaufmann: Washington, DC, 1989; pp 42−50. (c) Deb, K.; Pratap, A.; Agrawal, S.; Meyarivan, A. Fast and Elitist Multi-objective Genetic Algorithm: NSGAII. T. *IEEE Trans. EVol. Comput.* **2002,** *6,* 182–197. (d) Kalyanmoy, D. *Multi-ObjectiVe Optimization using Evolutionary Algorithms*; John Wiley & Sons: West Sussex, U.K., 2001.

(13) Zhang, D.; Yoshida, D.; Oekermann, T.; Furuta, T.; Minoura, K.; Room-Temperature, H. Synthesis of Porous Nanoparticulate TiO_2 Films for Flexible Dye-Sensitized Solar Cells. *Adv. Funct. Mater.* **2006,** *16,* 1228–1234.

(14) (a) Muduli, S.; Lee, W.; Dhas, V.; Mujawar, S.; Dubey, M.; Vijayamohanan, K.; Han, S.-H.; Ogale, S. Enhanced Conversion Efficiency in Dye-Sensitized Solar Cells Based on Hydrothermally Synthesized TiO_2-MWCNT Nanocomposites. *Appl. Mater. Interf.* **2009,** *1,* 2030–2035. (b) Lee, T. Y.; Alegaonkar, P. S.; Yoo, J.-B. Fabrication of Dye sensitized Solar Cell Using TiO_2 Coated Carbon Nanotubes. *Thin Solid Films* **2007,** *515,* 5131–5135.

(15) (a) Liu, W.; Hu, L.; Dai, S.; Guo, L.; Jiang, N.; Kou, D. The Effect of the Series Resistance in Dye-sensitized Solar Cells Explored by Electron Transport and Back Reaction Using Electrical and Optical Modulation Techniques. *Electrochim. Acta* **2010,** *55,* 2338–2343. (b) Adachi, M.; Sakamoto, M.; Jiu, J.; Ogata, Y.; Isoda, S. Determination of Parameters of Electron Transport in Dye-Sensitized Solar Cells Using Electrochemical Impedance Spectroscopy. *J. Phys. Chem. B* **2006,** *110,* 13872–13880. (c) Bisquert, J. Theory of the Impedance of Electron Diffusion and Recombination in a Thin Layer. *J. Phys. Chem. B* **2002,** *106,* 325–333.

(16) (a) Zhang, D.; Yoshida, T.; Oekermann, T.; Furuta, K.; Minoura, H. Room-Temperature Synthesis of Porous Nanoparticulate TiO_2 Films for Flexible Dye-Sensitized Solar Cells. *Adv. Funct. Mater.*

2006, *16*, 1228–1234. (b) Longo, C.; Nogueira, A. F.; De Paoli, M. A.; Cachet, H. Solid-State and Flexible Dye-Sensitized TiO_2 Solar Cells: a Study by Electrochemical Impedance Spectroscopy. *J. Phys. Chem. B* **2002,** *106*, 5925–5930.

(17) Hore, S.; Vetter, C.; Kern, R.; Smit, H.; Hinsch, A. Influence of Scattering Layers on Efficiency of Dye-sensitized Solar Cells. *Sol. Energy Mater. Sol. Cells* **2006,** *90*, 1176–1188.